

Improvement of scattering correction for in situ coastal and inland water absorption measurement using exponential fitting approach*

YE Huping (叶虎平)^{1,2,3,4}, LI Junsheng (李俊生)¹, ZHU Jianhua (朱建华)³,
SHEN Qian (申茜)¹, LI Tongji (李铜基)³, ZHANG Fangfang (张方方)¹,
YUE Huanyin (岳焕印)⁵, ZHANG Bing (张兵)^{1,2,**}, LIAO Xiaohan (廖小罕)^{5,**}

¹ Institute of Remote Sensing and Digital Earth, Chinese Academy of Sciences, Beijing 100094, China

² University of Chinese Academy of Sciences, Beijing 100049, China

³ National Ocean Technology Center, Tianjin 300112, China

⁴ Sino-Africa Joint Research Center, Chinese Academy of Sciences, Wuhan 430074, China

⁵ State Key Laboratory of Resources and Environmental Information System, Institute of Geographic Sciences and Natural Resources Research, Chinese Academy of Sciences, Beijing 100101, China

Received Feb. 11, 2017; accepted in principle Apr. 12, 2017; accepted for publication Jul. 3, 2017

© Chinese Society for Oceanology and Limnology, Science Press and Springer-Verlag GmbH Germany, part of Springer Nature 2018

Abstract The absorption coefficient of water is an important bio-optical parameter for water optics and water color remote sensing. However, scattering correction is essential to obtain accurate absorption coefficient values in situ using the nine-wavelength absorption and attenuation meter AC9. Establishing the correction always fails in Case 2 water when the correction assumes zero absorption in the near-infrared (NIR) region and underestimates the absorption coefficient in the red region, which affect processes such as semi-analytical remote sensing inversion. In this study, the scattering contribution was evaluated by an exponential fitting approach using AC9 measurements at seven wavelengths (412, 440, 488, 510, 532, 555, and 715 nm) and by applying scattering correction. The correction was applied to representative in situ data of moderately turbid coastal water, highly turbid coastal water, eutrophic inland water, and turbid inland water. The results suggest that the absorption levels in the red and NIR regions are significantly higher than those obtained using standard scattering error correction procedures. Knowledge of the deviation between this method and the commonly used scattering correction methods will facilitate the evaluation of the effect on satellite remote sensing of water constituents and general optical research using different scattering-correction methods.

Keyword: absorption coefficient; scattering correction; AC9/ACS; exponential fitting method

1 INTRODUCTION

Light absorption by particulate material and dissolved organic matter is an important source of optical variability in ocean and inland surface water. This variability consequently affects light attenuation, primary production, remote sensing of phytoplankton biomass, and mixed-layer heating (Sosik and Mitchell, 1995; Bricaud et al., 2004; Kirk, 2010; Zhang et al., 2014). The light absorption properties of an aquatic medium are characterized by the absorption coefficient. Absorption coefficient a , scattering coefficient b , and attenuation coefficient c ($c=a+b$)

are basic inherent optical properties (IOPs) of water that depend only on the medium and are independent of the ambient light field within the medium (Mobley, 1994). Although a is defined in terms of the behavior

* Supported by the National Key Research and Development Program of China (Nos. 2016YFB0501502, 2016YFC1400903, 2016YFB0500304), the National Natural Science Foundation of China (Nos. 91638201, 41276184, 41325004, 41471308, 41571361), the High Resolution Earth Observation Systems of National Science and Technology Major Projects (No. 41-Y20A31-9003-15/17), and the Director Foundation of Institute of Remote Sensing and Digital Earth, Chinese Academy of Sciences (No. Y6SJ2100CX)

** Corresponding authors: zb@radi.ac.cn; liaoxh@igsrr.ac.cn

of light passing through an infinitesimal volume of a medium, its value can nevertheless be obtained from the observed absorbance of the layer of a medium with finite thickness provided that the scattering effects can be overcome (Kirk, 2010). Instruments specifically designed to measure a of surface water bodies, e.g., marine or inland, are referred to as absorption meters. The methods generally used to measure a of water involve collecting water samples at field stations and then analyzing them in laboratories using spectrophotometers (Roesler, 1998) or deploying meters in situ for water displacement measurement in profiling, moored, autonomous underwater vehicles, or towed applications. The widely adopted in situ instrument is the Western Environmental Technologies Laboratories (WET Labs) reflecting-tube nine-wavelength absorption and attenuation meter AC9 (or its hyper-spectral successor ACS) (Moore et al., 1992; Zaneveld et al., 1994; Twardowski et al., 1999; Sullivan et al., 2006). The reflective tube design uses a quartz tube and a diffuser in front of a large-area receiver. Consequently, the reflective-tube collects forwardly scattered light from the total reflection at the tube walls when light is scattered at angles smaller than the angle of total reflection, i.e., approximately 41.7° (Zaneveld et al., 1994). Most particle scattering is in the forward direction, which makes the reflective-tube design quite effective in water. However, some of light scatters at wider angles than 41.7° , which leads to systematic overestimation of a . The uncollected light leads to an error in the determination of the absorption coefficient, which is called “scattering error.”

Various scattering correction schemes based on different assumptions have been proposed to correct the absorption measurements for scattering errors, such as the following: (1) The flat method (Zaneveld et al., 1994) involves subtracting the measured absorption at a near-infrared (NIR) reference wavelength where the absorption is assumed to be zero, e.g., $\lambda_{\text{NIR}}=715$ nm for AC9 or $\lambda_{\text{NIR}}=750$ nm or a longer band for measurements using a laboratory spectrophotometer. (2) The fixed-proportion method or Kirk method (Kirk, 1992) involves removing a fixed proportion (denoted by ε) of b , which is computed by subtracting a from c , where the volume scattering function (VSF) is assumed to be wavelength independent and without an NIR reference band. ε varies from approximately 0.14 for predominately biological particles in the open ocean (Case 1 water) to approximately 0.18 in waters where the scattering

is predominantly due to suspended sediments (Case 2 water) (Pegau et al., 2003). (3) The varied proportional scattering correction method or Zaneveld method (Zaneveld et al., 1994), which is a standard method, assumes that a reference wavelength exists where a is negligible for particulate and dissolved materials. The VSF shape is independent of the wavelength. This technique allows for automatic changes in the scattering correction magnitude with wavelength and changes with the types of materials present (Pegau et al., 2003). The flat and Zaneveld methods, which are described in the National Aeronautics and Space Administration (NASA) Ocean Optics protocols (Pegau et al., 2003) and version Q of the AC meter protocol (2011), were the most commonly used methods in the past. They could provide reasonably good results in coastal waters for shorter wavelengths only but underestimate the absorption at longer wavelengths due to non-zero NIR absorption that invalidates the assumption (Röttgers et al., 2013). Several new approaches have been proposed in recent years to overcome and improve the earlier methods. (4) The iterative scattering correction method or McKee method (McKee et al., 2008, 2013) uses an iterative scattering correction scheme based on Monte Carlo simulations of the WET Labs AC9 optical layout, employing additional backscattering measurements to estimate the backscattering. (5) In the “true” value empirical method or Röttgers method (Röttgers et al., 2013), a laboratory-based point source integrating cavity absorption meter (PSICAM) is used to avoid scattering errors and to develop an empirical relationship between the “true” absorption at 715 nm and the AC9 offset-error-measured absorption at 715 nm. This correction method divides the attenuation by 0.56 to correct for acceptance angle effects. This method is employed to evaluate the absorption in coastal waters using AC9 meters by applying scattering corrections to the flat and Zaneveld methods. (6) The exponential fitting method or Boss method (Boss et al., 2013) assumes that the absorption spectra are dominated by non-algal particles (NAPs) in the Dead Sea where the spectra are nearly exponentially decreasing (with an unknown slope). A best-fit power law relationship is obtained by performing nonlinear least-squares minimization using measurements at the seven shortest AC9 wavelengths to find the scattering contribution by applying scattering correction to all of the absorption bands. The seven wavelengths are used, to avoid temperature and salinity effect in this fitting, as these

are strongest for the last two wavelengths. Several other scattering correction methods have been proposed for WET Labs AC9 absorption data, such as using Monte Carlo modeling to examine residual scattering losses theoretically (Leymarie et al., 2010).

Inland and coastal Case 2 waters obviously exhibit absorption at wavelengths longer than 700 nm due to higher concentrations of detritus (Tassan and Ferrari, 2003; Röttgers et al., 2014). Therefore, the assumption that the absorption at 715 nm is zero in the flat and Zaneveld methods is invalid. Kirk's value of $\epsilon \approx 0.18$ for turbid waters is apparently not suitable for changeable Case 2 waters. The McKee method requires concurrent measurements of particulate backscattering to facilitate estimation of the scattering phase function as a part of the iterative correction process and to obtain effective percentage reflectance efficiency r_w for photons at the flow-tube wall. However, concurrent backscattering data are not necessarily available in historical absorption data sets, and r_w is time dependent and differs among AC9 units. Meanwhile, the Röttgers method (Röttgers et al., 2013) has not been fully validated under different water types due to the limited availability of PSICAM technology in the community. The Boss method (Boss et al., 2013) is suitable for waters dominated by inorganic particulate matter. However, due to the existence of chlorophyll (Chl) *b* and other pigments in phytoplankton in natural water, their 650 nm absorption peaks (Bidigare et al., 1990; Sosik and Mitchell, 1995) significantly affect the data fitting in the 650 nm band. Sokoletsky and Shen (2014) observed that different scattering corrections to AC9 absorption measurements vary by up to 30% in remote sensing reflectance models. Therefore, it is important to assess the variance among the main scattering correction approaches.

We modified Boss' method into a technique that we termed as exponential method for application to in situ coastal and inland waters to avoid the zero-absorption assumption in the NIR band and improve the underestimation in the red band that occurred in the standard scattering correction methods for Case 2 water absorption measurements. In addition, different scattering correction methods on the AC-9/ACS data were compared, and the error statistics for each water sampling type were calculated. The results from four typical water-sampling cruises obtained using these methods are presented in this paper. The exponential method is potentially suitable for retrospective application to historical data sets without requiring any additional data.

2 MATERIAL AND METHOD

2.1 Sample collection and analysis

For this study, Case 2 water samples were collected from a variety of sources: an estuary, a gulf, a lake, and reservoir water. In total, 103 surface samples were collected during four ship cruises: a cruise in the estuary of the Changjiang (Yangtze) River and its adjacent coastal area in the East China Sea on March 21–29, 2012 (CJK cruise) (Zhu et al., 2014); a cruise in the Liaodongwan Gulf in the Bohai Sea on July 14–19, 2011 (LDW cruise); a cruise on Lake Taihu on May 10–12, 2013 (TH cruise); and a cruise in the Guanting Reservoir on August 15, 2015 (GT cruise; see Table 1 and Fig.1). Remote sensing reflectance $R_{rs}(\lambda)$ in the sample stations cover four of the five types of Chinese coastal waters, which range from eutrophic to very turbid waters, and can be categorized as follows according to previous research results: phytoplankton and colored dissolved organic matter (CDOM) co-dominant waters, mixed waters with no dominant components, total suspended matter (TSM)-dominant waters, and water with very high suspended sediment concentrations. Samples of phytoplankton-dominant or oligotrophic water were not collected (Ye et al., 2016). $R_{rs}(\lambda)$ measurements were also obtained from three types of inland water: highly mixed eutrophic water, relatively clear water dominated by CDOM, and water dominated by non-living solids (Shen et al., 2015).

The data and measurement methods adopted for R_{rs} , a , absorption by CDOM or yellow matter a_g , absorption by particles a_p , b , and c , TSM concentration, NAP concentration, and phytoplankton (Chl *a*) concentration have been systematically described in the papers of Ye et al. (2016), Shen et al. (2015), and Zhu (2003). Their works are briefly reviewed below.

The coastal waters were measured using a 25-cm path-length tube AC9 [Serial No. (SN): ac90309] and

Table 1 Ranges (minimum–maximum) of TSM, NAP, and Chl concentrations and CDOM absorption at 440 nm for the four data sets (CJK, LDW, TH, and GT)

	CJK	LDW	TH	GT
TSM (g/m ³)	7–58	3–27	33.31–160.93	5–18.39
NAP (g/m ³)	4.67–46	1.56–10	17.5–138.4	0.86–8.77
Chl <i>a</i> (mg/m ³)	0.158–2.174	2.20–18.11	12.02–73.78	20.25–47.62
CDOM (/m)	0.029–0.131	0.11–0.32	0.96–2.07	0.65–0.95

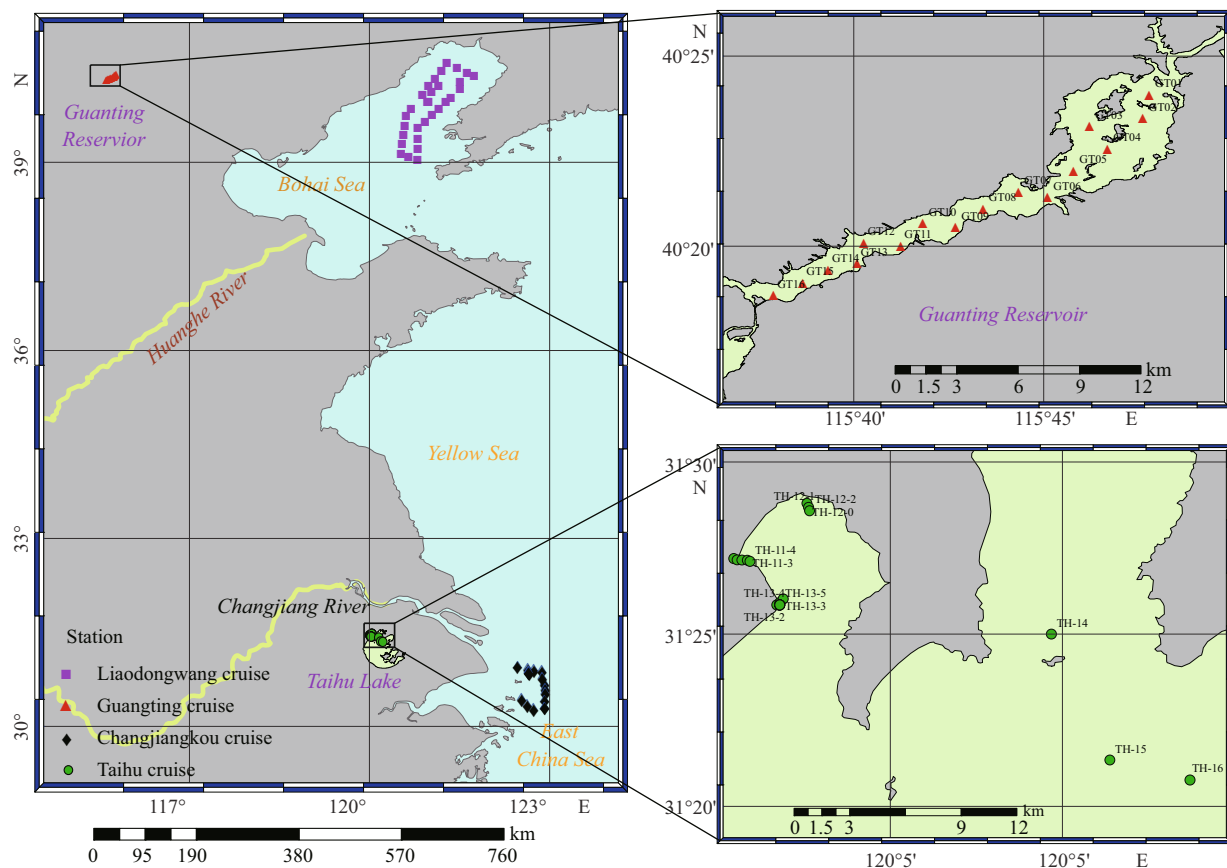


Fig.1 Sampling positions during the different cruises: CJK, LDW, TH, and GT cruises

an ACS (SN: acs061). The inland waters were measured using a 10 cm path-length tube AC9 (SN: ac90320) and an ACS (SN: acs173). The data were strictly obtained according to NASA Ocean Optics protocols for satellite ocean color sensor validation (Twardowski et al., 1999) and WET Labs AC meter protocol document (Version Q, 2011). The AC meter was regularly calibrated in the laboratory using bubble-free pure water (Milli-Q) before, during, and after the field campaigns. The calibration values were obtained by averaging a and c over a period of at least 45 s. The temperature of the outflow water was measured to enable temperature-dependent water absorption corrections to be applied. The entire process was repeated for three or more times until the replicated calibration values of each wavelength in each channel were within $\pm 0.003/\text{m}$ of one another. The values of a and c were measured by profiling three times at a speed of less than 0.3 m/s to avoid the “time-lag” effect (the time required for a sample to transit from the intake, through the filter, into the flow tube, and finally to be measured) in the coastal cruises using Data Handler (DH4, WetLabs) software. During the inland cruises, the measurements were conducted

over 60 s periods using WETView 7.0 (WetLabs) software. Simultaneously, conductivity, temperature, and depth (CTD) measurements were performed to obtain temperature and salinity profiles. The water samples in each station were collected and stored, and the absorption parameters such as a , a_g , and a_p were measured using the quantitative filter technique (QFT) using a UV/VIS Cintra20 spectrophotometer (GBC Scientific Equipment, Australia) (Bidigare et al., 1990; Roesler, 1998). Sample filter paper, namely, GF/F, with a diameter of 25 mm and a pore size of approximately 0.7 μm , was presoaked in 0.2 μm filtered seawater for 30 min and used to filter particles at 120–140 mm Hg negative pressure. A Cintra 20 spectrophotometer was used to measure the optical absorbance spectra of particles [$\text{OD}_{\text{p}}(\lambda)$] and blank filter (OD_{null}). The absorbance spectrum was interpolated to 1 nm wavelength resolution. A mean optical density of 11 nm, selected from 790 to 800 nm, was set as zero for null correction of the absorption values. The correction factors of Pegau et al. (2003) were used for the optical path-length amplification to calculate absorption coefficients using the formula $a_p(\lambda) = 2.303A[\text{OD}_{\text{p}}(\lambda) - \text{OD}_{\text{null}}]/(V/\beta)$ and for further

determination of the absorption coefficients of total particles [$a_p(\lambda)$], where A represents the effective filter surface area (cm^2) of suspended particles, V represents the sample volume (mL) of sample solution, and β represents the correction factor of amplified optical path-length. For $a_g(\lambda)$, the water samples were first filtered using Millipore membrane filters with a 0.2- μm pore size to remove the particulate materials. The null correction for $a_g(\lambda)$ absorption values was selected as the mean value from 690 to 700 nm (Zhu, 2003). The accuracy of the spectrophotometer measurements of particles $a_p(\lambda) < 6\%$ and yellow matter $a_g(\lambda) < 10\%$ was determined by calculating the average relative error in the visible bands by measuring replicated samples (each with multiple measurements). The Chl a concentrations were measured by using a spectrophotometer after the water samples had been filtered through 47 mm diameter filters (membrane filter with pore size of 0.7 μm). For the TSM and NAP measurements, the water samples were filtered using the previously weighed GF/F filters. The filters were dried at 105°C for 24 h, weighed in the laboratory, and then combusted for 4 h at 550°C and weighed again. TSM was assumed as the difference between the weight of the dried material and the initial weight of the unused filter, whereas NAP was assumed as the weight of combusted material (Pegau et al., 2003). $R_{rs}(\lambda)$ was measured following the above-water methods described in the Ocean Optics protocol (Mueller et al., 2003) using an ASD FieldSpec spectroradiometer.

Since the AC9 and ACS measurements were referenced to blank values calibrated using pure water, the measured a and c values represent the absorption and attenuation of all of the materials, respectively, except for the water in each sample due to the

subtraction of the latest pure water calibration data (i.e., the removal of a and c for pure water). The temperature and salinity effects were largest in the NIR region and were negligible in the visible region. The salinity and temperature effects on the seawater samples and temperature effect on the inland freshwater samples (where the salinity is near zero and therefore negligible) on the absorption and attenuation of pure water were removed following the recommended procedure using the temperature and salinity correction coefficients given by Pegau et al. (1997) for AC9 measurements and by Sullivan et al. (2006) for ACS measurements. In the following, absorption coefficient $a_m(\lambda)$ and attenuation coefficient $c_m(\lambda)$ represent the measurements obtained after applying pure water, temperature, and salinity corrections, and the absorption coefficients obtained after applying the scattering corrections are denoted as $a(\lambda)$.

2.2 Method

2.2.1 Flat, Kirk, Zaneveld, and Röttgers methods

See Table S1.

2.2.2 Exponential-fitting method or exponential method

The exponential method is a modification of the Boss method (Boss et al., 2013). The absorption spectrum is expected to be dominated by particles and yellow matter and is close to decreasing exponential function $a(\lambda) = a(440)e^{-S_p(\lambda-440)}$ (Babin et al., 2003; Morel, 2009). In the Zaneveld method, a constant proportion of the scattering is removed from the absorption (Zaneveld et al., 1994). The magnitude of ε , which is a wavelength-independent quantity, is used to measure non-water absorption by performing the following fit to the measured absorption spectra $a_m(\lambda)$ using an

Table S1 Flat, Kirk, Zaneveld, and Röttgers methods

Format	Method	Assumption and reference λ_r
	Flat method (Zaneveld et al., 1994)	$c_m(\lambda) - a_m(\lambda) \equiv c_m(\lambda_r) - a_m(\lambda_r)$ AC9: $\lambda_r = 715$ nm ACS: $\lambda_r = \text{last band in NIR}^*$
$a(\lambda) = a_m(\lambda) - a_m(\lambda_r) \frac{[c_m(\lambda) - a_m(\lambda)]}{[c_m(\lambda_r) - a_m(\lambda_r)]}$	Kirk method (Kirk, 1992)	$\frac{a_m(\lambda_r)}{c_m(\lambda_r) - a_m(\lambda_r)} \equiv 0.14$ for clear water or 0.18 for turbid water
	Zaneveld method (Zaneveld et al., 1994)	AC9: $\lambda_r = 715$ nm ACS: $\lambda_r = \text{last band in NIR}^*$
$a(\lambda) = a_m(\lambda) - (a_m(715) - a_m(715)) \frac{[(1/e)c_m(\lambda) - a_m(\lambda)]}{[(1/e)c_m(715) - a_m(715)]}$	Röttgers method (Röttgers et al., 2013)	$e_c = 0.56$ $a(715) = 0.212 \times a_m(715)^{1.135}$

*: the minimum value generally appears in the last band where the acs061 last band is 726 nm and the acs173 last band is 736 nm.

implicit model: $a(\lambda)=a_m(\lambda)-\varepsilon(c_m(\lambda)-a(\lambda))$ or $a(\lambda)=\frac{a_m(\lambda)-\varepsilon c_m(\lambda)}{1-\varepsilon}$. Although the attenuation error caused by the lens-aperture system has long been understood (Zaneveld et al., 1994), no consensus was arrived at within the community on an appropriate scattering correction, and $c_m(\lambda)$ has generally been left uncorrected. Corrected absorption $a(\lambda)$ is given by $a(440)e^{-S_p(\lambda-440)}(1-\varepsilon)+\varepsilon c_m(\lambda)=a_m(\lambda)$.

A nonlinear least-squares minimization technique is used in seven AC9 wavelengths (412, 440, 488, 510, 532, 555, and 715 nm) to obtain three unknowns: $a(440)$ (/m), S_p (/nm), and ε . Using the obtained value therefore of ε , $a(\lambda)$ is obtained by $a(\lambda)=\frac{a_m(\lambda)-\varepsilon c_m(\lambda)}{1-\varepsilon}$. Similar to $a_{pg}(\lambda)$, $a(\lambda)$ represents the sum of the absorption coefficients due to particles $a_p(\lambda)$ and yellow matter $a_g(\lambda)$. The Boss method uses the seven shortest AC9 wavelengths to avoid the potential necessity of error correction under extreme temperature and salinity conditions (e.g., in the Dead Sea, where the parameters are out of the CTD range). The method presented here for AC9 is generally applicable to the hyper-spectral version of the instrument (ACS) using the same seven wavelengths.

3 RESULT

Using the five scattering correction methods (flat, Zaneveld, Röttgers, exponential, and Boss methods) and applying them to the four cruise data sets acquired by the AC9/ACS, we analyzed and evaluated the exponential method. We compared our exponential method with the standard Zaneveld method in various bands and cruises, evaluated the correction effects relative to those of other scattering correction methods in all the bands, and validated the corrected data with the $a_p(\lambda)$ and $a_g(\lambda)$ data acquired using a laboratory spectrophotometer.

3.1 AC9/ACS scattering correction

3.1.1 Application of exponential scattering correction method to AC9 measurements

The water sample from the CJK-01 station is turbid (TSM=42 g/m³, NAP=34.7 g/m³, and Chl *a*=0.24 mg/m³), and the raw absorption spectra are dominated by NAPs. The spectra are nearly exponentially or linearly decreasing, and without peaks at 676 nm (in contrast to those from the TH-10-0 station; see below). After application of the scattering correction (Fig.2a), the a_{pg} values calculated using the exponential method

are larger than those derived using the Zaneveld method. The values lie between those calculated using the flat and Zaneveld methods in the blue and green bands (≤ 600 nm). However, they are larger than the results obtained using these two methods in the red and NIR bands (>600 nm). The absorption values calculated using the exponential method do not tend to zero at long wavelengths, and they are smaller than those of the Röttgers method across the entire range.

The water sample from the TH-10-0 station is eutrophic and turbid (TSM=33.31 g/m³, NAP=18.06 g/m³, and Chl *a*=49.86 mg/m³), and the raw absorption spectra are dominated by NAPs in the short band and Chl *a* in the long band. The absorption coefficient spectra are nearly decreasing exponentials or linear in the blue and green bands (≤ 600 nm). They also exhibit small peaks at 676 nm. The results of the application of the exponential scattering-correction method to the data from the TH-10-0 station, which are shown in Fig.2c, show behavior similar to that of the CJK-01 results. The exponential method results are close to those obtained using the flat method.

The analysis of the values obtained after applying the scattering corrections to the CJK and TH cruise data are described in Section 3.3. The absorption coefficients determined from the CJK cruise station data vary from 0.18 to 1.96/m in the 412 nm band after correction using the exponential method. These results are shown in Fig.2b. The R_{rs} values of these station peaks at 490, 500–550, 565, and 570 nm or longer correspond to the phytoplankton and CDOM co-dominant waters, mixed waters with no dominant components, TSM-dominant waters, and very high suspended sediment concentrations in water, respectively, which are the most common types of coastal water (Zhu et al., 2014; Ye et al., 2016). The absorption values obtained from the TH cruise samples are obviously larger than those from the coastal cruise [$a(412)>3.7$ /m], as shown in Fig.2d. The dominant three water types here are water dominated by NAPs [$a(412)>10$ /m], eutrophic water [$a(676)>2$ /m], and ordinary water (with a low peak at 676 nm). The TH absorption coefficients, similar to those obtained from the CJK cruise data, are nearly decreasing exponentials or linear but are much larger than those from the CJK cruise, which suggests that the water is dominated by NAPs (and CDOM) with high concentrations. The other water types show peaks at 676 nm, which suggest that the absorption due to phytoplankton in these water types is dominant in this band.

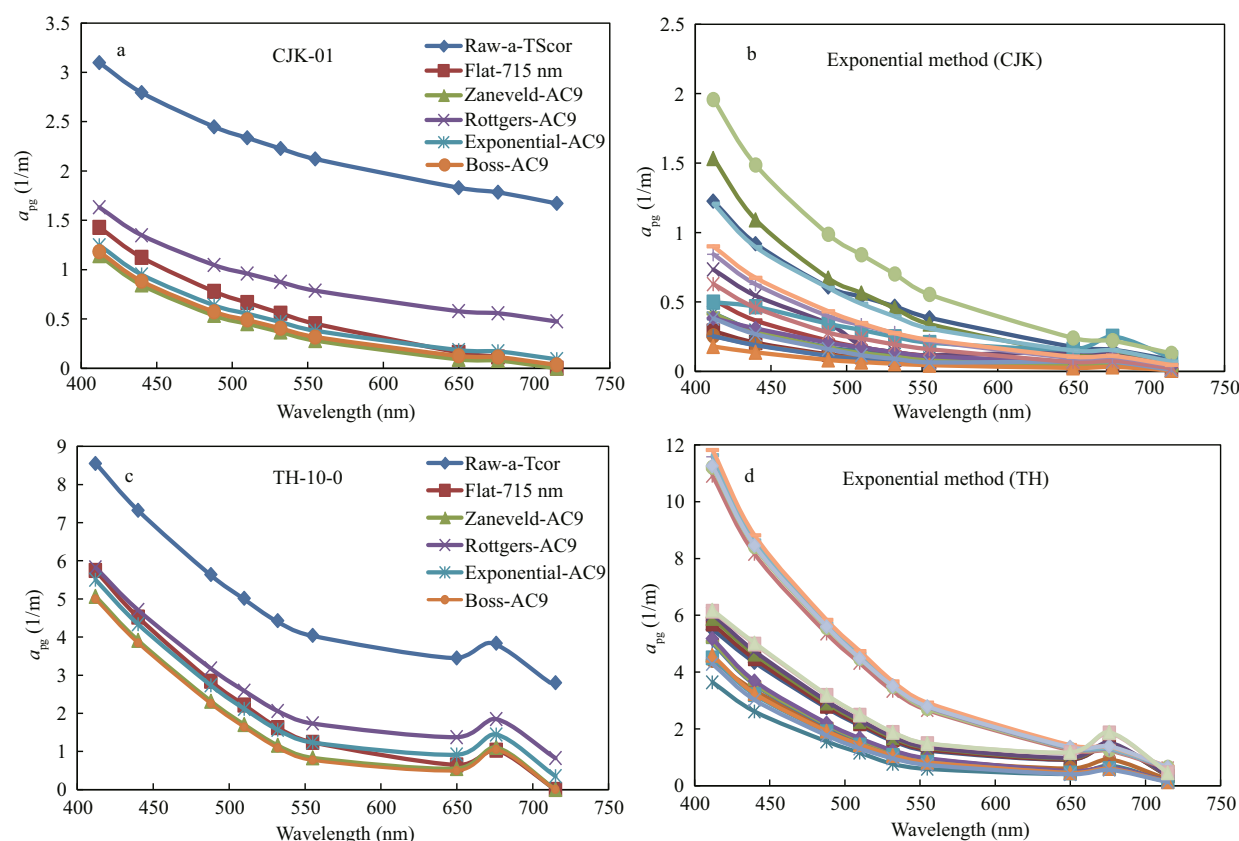


Fig.2 Application of the five scattering correction methods to the AC9 data

a. corrected data from the CJK-01 station (25 cm path-length tube) in the estuary of the Changjiang River and its adjacent coastal area; b. results of applying exponential scattering corrections to all the CJK cruise data; c. corrected data from the TH-10-0 station (10 cm path-length tube) in Lake Taihu; d. results of applying exponential scattering corrections to all the TH cruise data.

3.1.2 Application of exponential scattering correction method to ACS measurements

The exponential method for AC9s is generally applicable to the hyper-spectral version of the same instrument (ACS), and the characteristics of the ACS absorption spectra are described below. The raw absorption spectra from the LDW-03 station ($TSM=6.7 \text{ g/m}^3$, $NAP=6.0 \text{ g/m}^3$, and $Chl a=2.45 \text{ mg/m}^3$) are nearly decreasing exponentials with weak dips at 450 nm and small peaks at 650–700 nm. The results of the exponential scattering correction method are compared with those of the other three scattering correction methods and shown in Fig.3a. The values generated using the exponential method closely approximate those obtained using the flat method in the blue and green bands ($\leq 600 \text{ nm}$). The results of applying the exponential scattering corrections to all the LDW data are shown in Fig.3b.

In the GT-01 station, the water is eutrophic ($TSM=10 \text{ g/m}^3$, $NAP=4.44 \text{ g/m}^3$, and $Chl a=47.62 \text{ mg/m}^3$). In this case, the raw absorption spectra are strongly influenced by the absorption of algal

particles, as shown in Fig.3c. These spectra are neither decreasing exponentials nor linear and show small peaks at 440, 490, 632, and 676 nm caused by the absorption of most types of phytoplankton pigments (Hoepffner and Sathyendranath, 1991). In contrast, the absorption spectra in case of the reservoir upstream water are relatively smooth, as shown in Fig.3d, where the only remaining obvious absorption peak occurs at 676 nm. The spectra remaining after applying the exponential scattering correction method retain the characteristics of the phytoplankton pigment absorption spectrum, and the values and shape are close to those resulting from the application of the Röttgers method. The absorption spectrum is not a decreasing exponential, which demonstrates that the exponential scattering correction method is relatively robust.

In summary, the corrected absorption values obtained using the exponential method are always between those of the flat and Zaneveld methods in the short band ($\leq 600 \text{ nm}$). The spectra exhibit values greater than zero in the red and NIR regions. The values are smaller than those obtained from the Röttgers method. We should note that the original

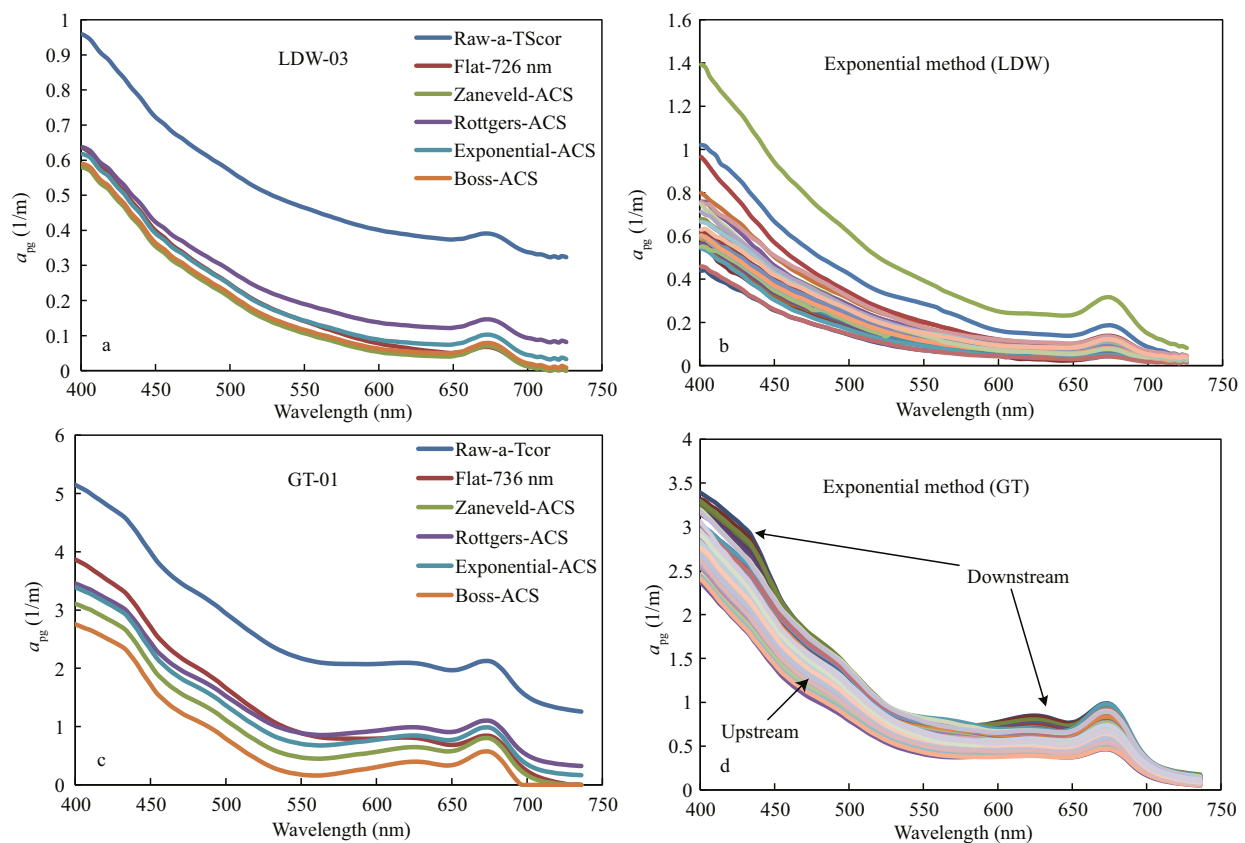


Fig.3 Absorption and attenuation coefficients of the measurements from the ACS meters after applying the scattering correction

a. corrected data from the LDW-03 station (25 cm path length) in the Gulf of Liaodongwang in Bohai Sea; b. results of applying exponential scattering corrections to all the data from the LDW cruise; c. corrected data from the GT-01 station (10 cm path length) in the Guanting Reservoir; d. results of applying exponential scattering corrections to all the data from the GT cruise.

absorption coefficients do not need to be exponentially decreasing. The values fit well for turbid, eutrophic, and ordinary Case 2 water types.

3.2 Comparison of the exponential and standard Zaneveld scattering correction results

The corrected scattering values obtained using the exponential and standard Zaneveld methods are compared, as shown in Fig.4. The values from the exponential method are always larger, and the relative variance is within -30% below the 555 nm band, whereas the variance is generally greater than -30% in the red and NIR bands. The bio-optical properties in the entire Guanting Reservoir are relatively uniform and similar. The absorption values only slightly vary and are relatively concentrated in a very narrow range. In the Zaneveld method, the correction is applied at the minimum NIR wavelength of 736 nm, which is the longest wavelength band in the ACS meter (SN: acs173). Consequently, all the values are greater than those in the NIR band at 715 nm. The absorption coefficients resulting from the exponential and

Zaneveld methods, therefore, are within 30% of each other. This finding supports the rationality of the exponential method to some extent. For the LDW cruise (SN: acs061), the minimum band selected for the Zaneveld method is the NIR band at 726 nm. Few moderate turbid water stations in the LDW cruise yield larger absorption values, as shown in Fig.3b, due to the existence of NIR absorption. The scattering-corrected values from the exponential method of the LDW station are close to those from the Zaneveld method and are within -30% in the red region. The difference between the results of the two methods is not significant or is negligible when the absorption coefficient is small because the absorption spectra between the NIR absorption coefficient of 715 nm and reference wavelength of 726 nm are flat. The results show that the values obtained using the exponential method in the red and NIR regions are larger than those derived using the standard Zaneveld method in the same regions. In the longer NIR reference band and at longer NIR wavelengths (refer to the TSM concentration), the results of the two scattering correction methods are in

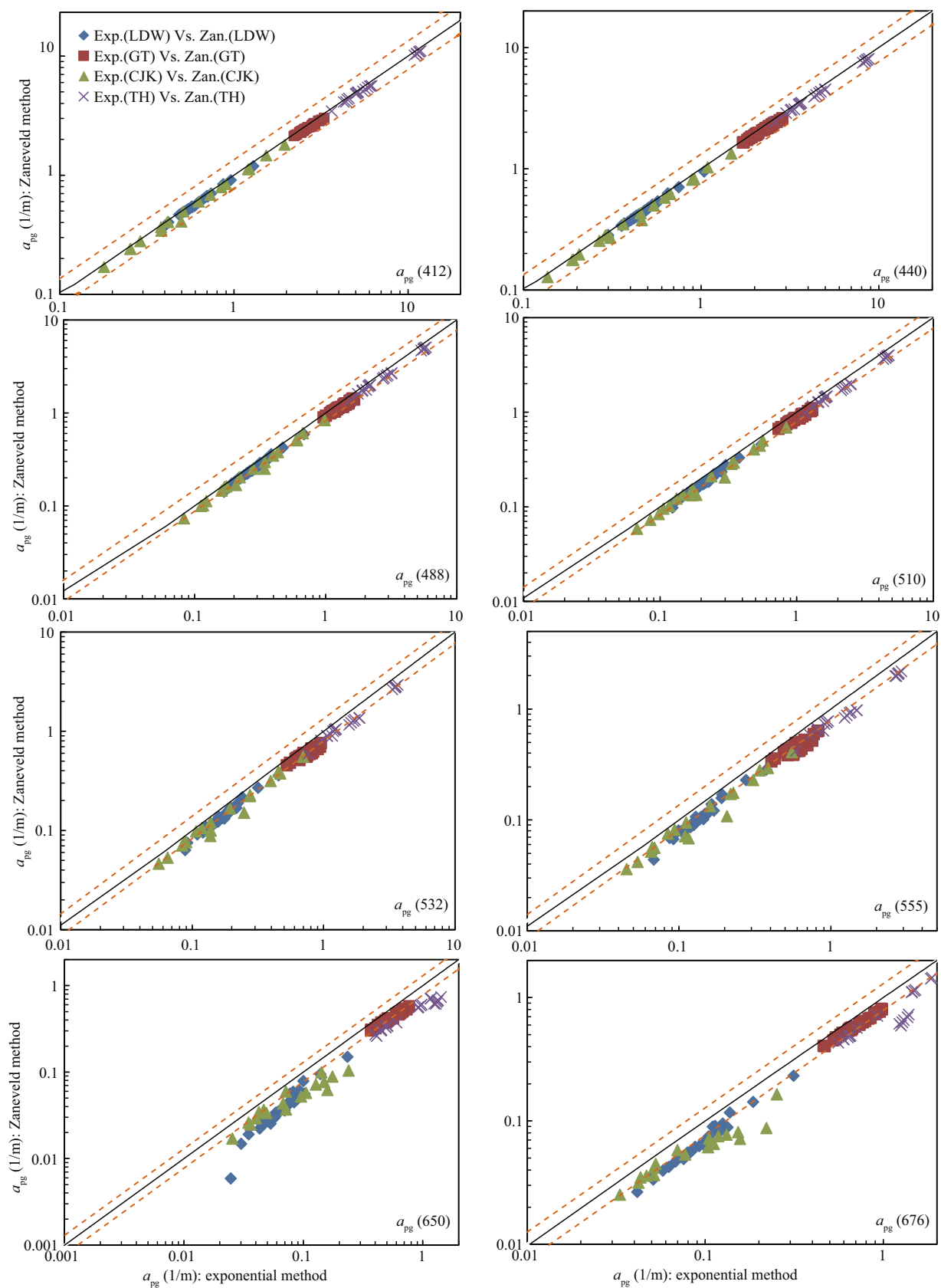


Fig.4 Comparison of the results obtained after applying the exponential and standard Zaneveld scattering correction methods for different cruises and bands

The solid lines are 1:1 lines, and the dashed lines are $\pm 30\%$ lines.

Table 2 Comparison of the median values (%) obtained from the exponential method and other scattering-correction methods (flat, Zaneveld, Röttgers, and Boss methods) (average, 95% confidence interval)

			412	440	488	510	532	555	650	676
Flat vs. exponential	95% confidence interval	Average	9.5	10.9	14.1	16.7	18.4	17.4	-11.6	-21.4
		Lower	7.3	8.0	10.2	12.1	13.3	11.7	-16.4	-23.7
		Upper	11.8	13.8	18.1	21.2	23.6	23.1	-6.9	-19.0
		Median	8.0	8.5	10.5	12.4	15.5	14.3	-14.0	-21.1
Zaneveld vs. exponential	95% confidence interval	Average	-5.8	-7.2	-11.6	-14.8	-19.4	-24.0	-34.9	-26.2
		Lower	-6.2	-7.7	-12.2	-15.6	-20.4	-25.2	-37.3	-28.4
		Upper	-5.4	-6.8	-11.0	-14.1	-18.4	-22.7	-32.5	-24.1
		Median	-5.4	-6.9	-11.4	-14.7	-19.1	-23.8	-33.4	-24.0
Röttgers vs. exponential	95% confidence interval	Average	8.7	13.1	23.9	31.9	42.6	54.1	91.0	74.7
		Lower	6.1	9.6	18.6	25.1	34.1	43.5	70.6	55.6
		Upper	11.2	16.6	29.3	38.7	51.2	64.7	111.3	93.8
		Median	3.4	5.3	12.7	17.9	24.5	32.6	34.5	23.4
Boss vs. exponential	95% confidence interval	Average	-8.7	-10.6	-17.3	-22.1	-29.2	-35.6	-42.7	-31.9
		Lower	-9.8	-11.9	-19.4	-24.8	-33.0	-40.2	-46.7	-34.9
		Upper	-7.6	-9.3	-15.1	-19.3	-25.4	-31.0	-38.6	-29.0
		Median	-7.5	-9.7	-15.4	-19.0	-23.1	-28.6	-46.3	-33.3

good agreement, which indicate that the exponential method works reasonably well.

3.3 Evaluation of the exponential method correction relative to those of other scattering correction methods

The flat and Zaneveld methods are the most widely applied and instrumentally recommended scattering correction methods and have been validated in multiple water types around the world. The disadvantages associated with these two methods are the invalid NIR zero-absorption assumption for Case 2 water and NIR overcorrection (McKee et al., 2013). In the Röttgers method, the experiential model developed based on measured data using PSICAMs without scattering errors is applied. This method has been verified in several European coastal areas and laboratory-cultured algae species (Röttgers et al., 2013). Although the general applicability and stability of this method are constrained by the limited applicability of empirical relationship at 715 nm using PSICAMs, it remains effective as a reference with which the exponential method can be compared. The exponential method is based on the Boss method developed for the Dead Sea, which is characterized by high salinity and high temperature. Sokoletsky and Shen (2014) suggested that different scattering corrections for AC9 absorption measurements can result in up to a 30% difference among the remote sensing reflectance models using radiative transfer.

Comparison of the exponential, flat, Zaneveld, Röttgers, and Boss methods is required to assess the correction effects of the exponential method. Furthermore, the deviations between the methods obtained from such comparisons could provide scientific references that would enable accurate analysis of the inverse algorithms for IOPs.

Because the flat and Zaneveld methods assume that the absorption coefficient is zero in the 715 nm band and the Boss method treats negative values as zeros, only the first eight visible bands of the nine bands measured by AC9s (the same bands that are measured by ACS meters) are discussed here. The results indicate that the corrected values from the exponential method are close to those from the flat. (average<20%) and Zaneveld (average>30%) methods in the blue-green bands (≤ 600 nm), as shown in Fig.5 and Table 2, with the values lying in between those of the flat and Zaneveld methods. However, the corrected values are generally higher than those of the flat and Zaneveld methods in the red and NIR bands (>600 nm). The corrected values obtained using the Röttgers method are close to those derived using the exponential method below the 510 nm band (median<18%; average<32%), but the average in each band is generally higher than that from the exponential method. The Zaneveld method yields the second-lowest corrected values among all methods. The Zaneveld method has been previously reported to produce underestimates in the red and NIR regions

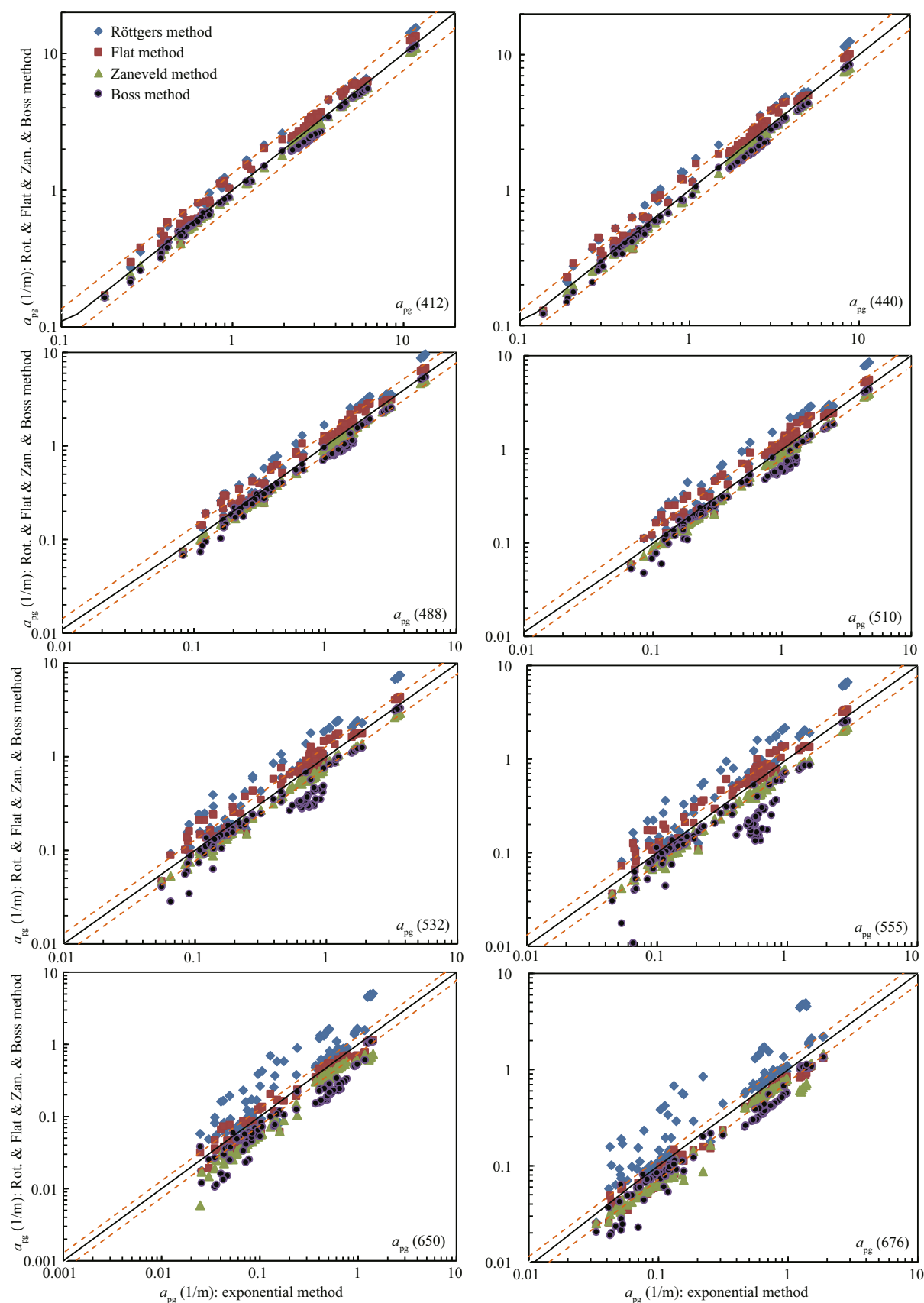


Fig.5 Comparison of the results of the exponential, flat, Zaneveld, Röttgers, and Boss methods

The black lines represent 1:1 lines, whereas the parallel brown dashed lines represent $\pm 30\%$ deviations.

(Doxaran et al., 2007; McKee et al., 2013; Röttgers et al., 2013; Sokoletsky and Shen, 2014). The Boss method yields the lowest corrected values among all methods. Compared with the results of the Zaneveld method, those of the Boss method are obviously overcorrected due to the influence of the absorption peak of phytoplankton and are close to the values in turbid water (Figs.2a, c, 3a). The corrected values from the Röttgers method are the highest in most of the green, red, and NIR bands. The corrected values obtained using the flat method are approximately equal to (or slightly higher than) those of the Röttgers method in the short band (412 nm) but are evidently lower than those from the exponential method in the long-wavelength and red-NIR regions (>600 nm). The corrected values derived from the Zaneveld and Boss methods are always lower than those from the exponential method.

The corrected values from each method are generally close to one another in the short band (e.g., the corrected values from all methods are concentrated within $\pm 10\%$ of the average or median values in the 412 nm band). However, as the wavelength increases, the corrected values obtained using the different methods begin to show discrepancies. The corrected values from the flat method are slightly higher than those from the exponential method in the short-band region. The corrected values from the Zaneveld method are always slightly lower than those from the exponential method. The corrected values from both the flat and Zaneveld methods are evidently lower than those from the exponential method in the bands longer than 600 nm. The absorption coefficients corrected using the Röttgers method are generally higher than those corrected using the exponential method with small differences in the short-band regions but more notable differences in the long-band regions.

3.4 Comparison of the corrected absorption coefficients obtained from the exponential method with using the laboratory spectrophotometer

AC measurement results are commonly applied in the development of semi-analytical algorithms and optical closure studies (Sokoletsky and Shen, 2014; Lefering et al., 2016). The measured values obtained via different methods/devices are comparable, just as measurement closure mentioned by Mobley (1994). a_{pg} , which is determined from AC9/ACS measurements, is equivalent to the summation of a_g and a_p . Figure 6a shows that the results from the

exponential method and the spectrophotometer are mostly concentrated near the 1:1 line [except for the values corresponding to 715 nm, which are relatively dispersed (Fig.6b)]. The values obtained using the exponential method are generally slightly higher than those measured by the spectrophotometer in the blue-green bands (<532 nm) and 676 nm (Table 3) (variance in median value <10%), indicating that the results of the exponential method are comparable with the spectrophotometer measurements and thus can be applied in optical closure studies. Multiple potential causes of the discrepancies between the values obtained using the two methods are present, such as the differences between the spectrophotometer and field measurement techniques. Absorption measurements using a spectrophotometer are affected by the path-length amplification effect (“ β effect”) and null correction. In this study, the null correction for yellow-substance absorption value $a_g(\lambda)$ was selected as the mean value from 690 to 700 nm (Zhu, 2003). The mean optical density of 11-nm, selected from 790 to 800 nm, was set as zero for the null correction of particle-absorption values $a_p(\lambda)$ in the transmittance (T) method to minimize the scattering error. However, the important uncertainties associated with the quantitative filter technique to determine the particulate absorption coefficient remain (Roesler, 1998). Moreover, some researchers found that the transmittance-reflectance method could improve the absorption coefficient measurement of the suspended particulate matter precision in highly turbid water (Tassan and Ferrari, 2002; Zhu et al., 2010; Shi et al., 2015). The difference between the depths where the water samples are acquired in the two methods is another important cause. The surface water samples used by the spectrophotometers are taken from 0 m or close to the 0 m surface, whereas in the field measurements, they are taken from depths of 0.5 or 1 m (sometimes, even 2.5 m) and are approximately treated as surface water samples.

The depth of the in-situ method is increased due to the structure of the instrument at the water inlet, which must be immersed beneath the water surface by approximately 0.5 m. In certain inland water types with significant layering distinctions, the difference between the water sample depths could cause the results of the two methods to be inconsistent. Therefore, we need to select water samples from the same layer in the water closure analysis and perform future algorithm development to reduce errors and improve the accuracy of error analysis.

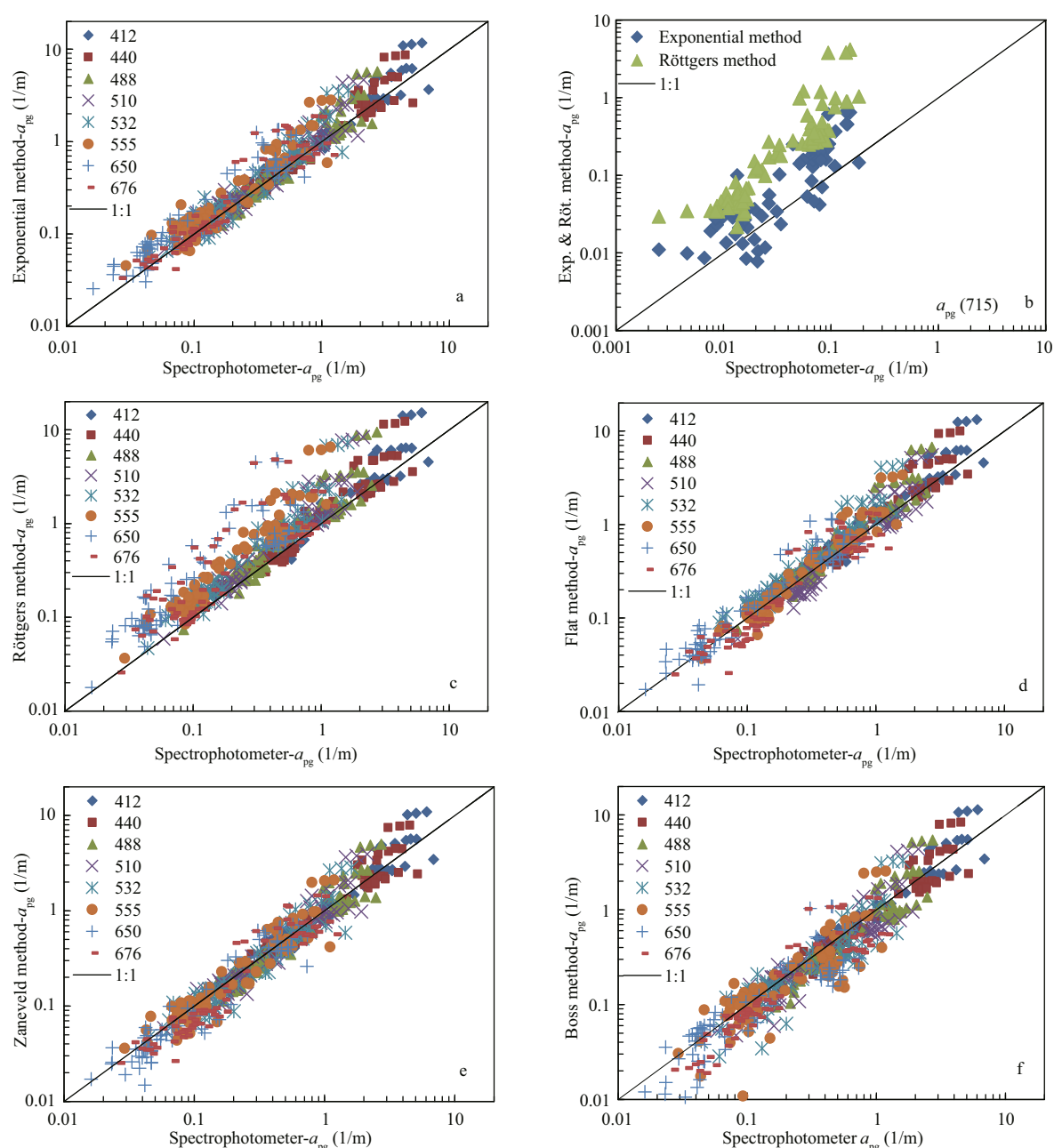


Fig.6 Comparison of the absorption results obtained using the laboratory spectrophotometer and the AC9/ACS with different scattering methods

The black diagonal line represents the 1:1 line.

4 DISCUSSION

4.1 Analysis of the influence of the fitting bands

The exponential method is a modified form of Zaneveld's proportional method (Zaneveld et al., 1994), which involves removing a constant proportion of the scattering from the absorption. The scattering contribution is obtained by generating a power law fit using nonlinear least squares minimization in the seven AC9 wavelengths among the types of water

with different dominant materials. It avoids assuming zero absorption in the NIR reference band. The scattering coefficient represents the difference between the measured attenuation and corrected absorption coefficients and approaches the true scattering value.

Boss et al. (2013) chose the seven shortest AC9 wavelengths to avoid the temperature- and salinity-sensitive bands (676 and 715 nm) and assumed that NAPs, whose spectra almost exponentially decrease,

Table 3 Comparison of the absorption values (%) obtained from the spectrophotometer and the AC9/ACS with different scattering-correction methods (flat, Zaneveld, Röttgers, exponential, and Boss methods) (average, 95% confidence interval)

			412	440	488	510	532	555	650	676
Flat vs. Spectrophotometer	95% confidence interval	Average	22.5	18.9	25.8	36.0	44.7	58.3	28.1	2.5
		Lower	13.7	9.1	14.4	24.2	32.8	45.6	15.7	-9.1
		Upper	31.3	28.7	37.3	47.9	56.7	70.9	40.4	14.2
		Median	17.2	10.8	13.7	24.6	31.9	45.1	14.4	-11.9
Zaneveld vs. Spectrophotometer	95% confidence interval	Average	5.9	-0.2	-1.2	1.8	2.9	8.3	-4.8	-4.7
		Lower	-1.2	-7.6	-9.5	-6.5	-5.3	-0.3	-12.9	-15.1
		Upper	13.1	7.2	7.0	10.2	11.1	17.0	3.3	5.7
		Median	-0.3	-8.9	-9.7	-5.4	0.1	7.5	-12.2	-18.5
Röttgers vs. Spectrophotometer	95% confidence interval	Average	23.2	23.5	40.6	58.5	79.5	113	195	156
		Lower	12.8	11.2	24.0	39.6	57.9	87.0	139	96.2
		Upper	33.5	35.8	57.1	77.3	101	140	251	216
		Median	14.7	10.4	20.0	34.8	55.1	85.3	119	52.3
Exponential vs. Spectrophotometer	95% confidence interval	Average	12.7	8.0	12.4	20.5	28.7	43.8	53.4	34.5
		lower	5.0	-0.2	2.8	10.4	18.1	31.9	39.2	18.3
		upper	20.3	16.1	22.0	30.5	39.3	55.8	67.6	50.6
		Median	5.2	1.0	1.2	9.9	22.8	38.7	48.4	9.6
Boss vs. Spectrophotometer	95% confidence interval	Average	4.4	-1.9	-4.2	-2.0	-2.8	1.0	-7.8	-6.4
		lower	-3.4	-10.0	-13.6	-12.1	-13.7	-11.3	-20.2	-19.5
		upper	12.1	6.2	5.2	8.1	8.0	13.3	4.6	6.6
		Median	-3.9	-11.4	-12.4	-10.4	-8.5	-1.8	-18.4	-20.2

dominated the water. The method met the absorption correction requirements of the Dead Sea, where the CTD measurements go out of range and cannot provide usable data. It may cause potential errors in ordinary Case 2 water, which has significant phytoplankton pigment absorption, e.g., Chl *b* has an absorption peak near 650 nm. In this study, we improved the fitting algorithm using measurements in seven AC9 wavelengths (412, 440, 488, 510, 532, 555, and 715 nm) to avoid the influence of the phytoplankton absorption peaks at 650 and 676 nm while also obtaining CTD measurements for temperature and salinity corrections in the red and NIR bands. The particulate absorption coefficient and its constituent contributions could be separated into algal absorption $a_{ph}(\lambda)$ and NAP absorption $a_d(\lambda)$, expressed as $a_p(\lambda) = a_{ph}(\lambda) + a_d(\lambda)$. The algal absorption coefficient is featured in spectra that are not exponentially decreasing. However, the concomitant NAP $a_d(\lambda)$ and yellow matter $a_g(\lambda)$ always exist in Case 2 water. They could be expressed by decreasing exponential function $a(\lambda) = a(440)e^{-S_p(\lambda-440)}$ in which

corresponding S_d and S_g are always unequal (Babin et al., 2003; Morel, 2009). The values of $a_d(\lambda)$ and $a_g(\lambda)$ can partially compensate for $a_{ph}(412)$ and cover the peak feature at $a_{ph}(440)$ in $a_{pg}(\lambda) = a_{ph}(\lambda) + a_d(\lambda) + a_g(\lambda)$. The absorption spectra without the 650 nm and 676 nm peaks were almost linear or exponentially decreased in the data obtained from the four cruises and in other coastal water types near the mainland of China, which are seriously influenced by suspended sediments (Ye et al., 2016). This result is similar to that found in the North Sea by Sullivan et al. (2016), which showed the North Sea absorption data sorted into six water “types” from algal (Chl *a*) dominated to more non-algal absorption dominated (a_{pg} magnitude), and in the Elbe River, Baltic Sea, and German Bight in the North Sea in the paper of Röttgers et al. (2013). Thus, the results agreed with the assumption of decreasing exponential functions. The raw absorption spectra were found to be not necessarily strictly decreasing exponential functions, similar to the case in the Guanting Reservoir water. We tested the chosen six or fewer AC9 wavelengths using the exponential

fitting method and found that ε was more discrete and irregular, especially outside the 412 nm band, for the four cruises than that in the exponential and Boss methods.

4.2 Variation in the magnitude of ε , spectral slopes of particulate, and CDOM absorption S_p

As previously mentioned, ε is a wavelength-independent quantity and is a measure of the contribution of the scattering to $a_{pg}(\lambda)$. In the Zaneveld method, $\varepsilon \in [0.117, 0.252]$. In the comparison, the values of ε obtained using the exponential and Boss methods are smaller, as shown in Fig. 7. In the exponential method, $\varepsilon \in [0.090, 0.197]$, and in the Boss method, $\varepsilon \in [0.092, 0.217]$. The ε values obtained using both these methods are within the scattering-corrected range of the AC instrument protocol, i.e., $\varepsilon \in [0.07, 0.35]$, and are consistent with the previous estimates (Zaneveld et al., 1994; Boss et al., 2013).

The scattering multiplied by ε in the Zaneveld method is related to uncorrected absorption $a_m(\lambda)$, whereas the scattering multiplied by ε in the Boss and exponential methods is directly related to corrected absorption $a(\lambda)$. The ε values of the exponential methods are relatively larger and are close to the true scattering error. Hence, the same scattering correction quantity corresponds to a smaller ε value. Because of the choice of the fitting band in the exponential method, which is not the same as that in the Boss method, the ε values are significantly different. In particular, in the Guanting Reservoir water, which has a relatively higher concentration of phytoplankton and pigment absorption at 650 nm, ε from the Boss method is obviously higher than that in the other

cruises with inorganic-dominated water, leading to absorption coefficient overcorrection, which is significantly lower than that from the Zaneveld method, as shown in Fig. 3c. The exponential method is also evidently stable and robust in most of natural water types, unlike the Boss method, which fails to produce accurate results in eutrophic water where the absorption spectra show pigment absorption characteristics. The ε values from the Boss method are generally higher than those from the exponential method, which cause the values in the corrected band to be significantly lower. Compared with the other two scattering correction methods, ε from the Boss method shows discrepancies and unstable behavior.

The exponential method particulate and CDOM absorption spectral slopes were found to be $S_p \sim 0.0083\text{--}0.0189/\text{nm}$ (median value: $S_p = 0.010463/\text{nm}$) and were observed to increase with increasing turbidity (Table 4). The S_p values from the exponential method are lower than those from the Boss method in all cruises. All results exhibit a typical Chl *a* absorption peak at 676 nm and a weak shoulder near 488 nm, such as the spectra in the Guanting Reservoir shown in Fig. 3d, which suggest that the photosynthetic organisms in the water column and phytoplankton dominated the water.

4.3 Method limitations and application conditions

$c_m(\lambda)$ in the exponential method was left uncorrected due to the lack of an appropriate standard scattering correction, although this error source has long been understood (Pegau et al., 2003), and attempts to solve it have recently been presented by Boss et al. (2009) using LISST and by McKee et al. (2013) using Bb9. The exponential method has been tested and analyzed in situ in several water types, excluding open ocean stations, clear inland water, and other extreme water types, which may significantly affect the choice of fitting bands in the exponential method. Thus, this method should be validated using samples of more water types that occur in natural complex coastal or inland water to enable further modification of the fitting algorithm and improvement in the scattering correction accuracy.

Sullivan et al. (2016) mentioned that approximately five to six commonly used correction methods had no community consensus, and their team remains committed to quantifying and improving the uncertainties (scattering error) in absorption measurements using AC devices in the NASA Plankton, Aerosol, Cloud, ocean Ecosystem (PACE)

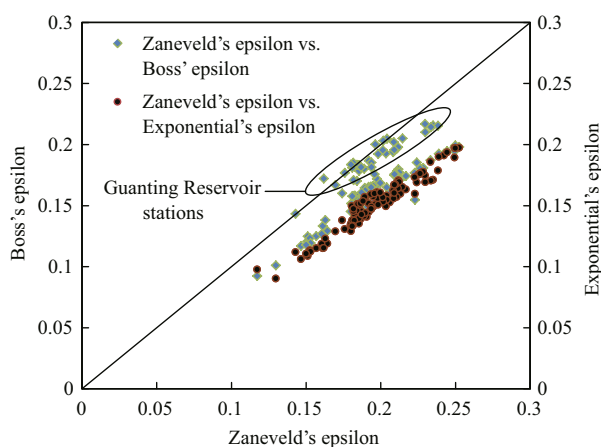


Fig. 7 Comparison of the ε values from the exponential, Zaneveld, and Boss methods

The black diagonal line represents the 1:1 line.

Table 4 Statistical values (minimum, maximum, median, and average) of the ϵ and S_p magnitudes from three scattering correction methods (Zaneveld, Boss, and exponential methods) in the four cruises

		Zaneveld- ϵ	Boss- S_p	Boss- ϵ	Exponential- S_p	Exponential- ϵ
LDW	Minimum	0.117 3	0.009 9	0.092 3	0.008 6	0.090 1
	Maximum	0.249 4	0.013 0	0.194 7	0.012 4	0.189 2
	Median	0.181 5	0.011 1	0.150 2	0.010 5	0.137 3
	Average	0.179 7	0.011 3	0.145 3	0.010 6	0.135 3
GT	Minimum	0.161 9	0.012 3	0.166 7	0.009 0	0.115 3
	Maximum	0.238 4	0.015 0	0.216 9	0.011 7	0.178 7
	Median	0.197 3	0.014 0	0.192 5	0.010 5	0.150 0
	Average	0.199 4	0.013 9	0.192 1	0.010 4	0.150 3
CJK	Minimum	0.162 9	0.008 9	0.138 1	0.008 3	0.122 9
	Maximum	0.197 4	0.016 8	0.175 6	0.012 5	0.160 7
	Median	0.186 2	0.011 6	0.158 7	0.010 2	0.151 5
	Average	0.185 7	0.011 9	0.159 5	0.010 2	0.150 7
TH	Minimum	0.181 0	0.009 8	0.156 8	0.009 5	0.133 0
	Maximum	0.252 5	0.019 3	0.199 2	0.018 9	0.197 3
	Median	0.222 7	0.012 8	0.177 1	0.011 6	0.169 3
	Average	0.217 3	0.013 2	0.178 0	0.012 2	0.169 6
All	Minimum	0.117 3	0.008 9	0.092 3	0.008 3	0.090 1
	Maximum	0.252 5	0.019 3	0.216 9	0.018 9	0.197 3
	Median	0.193 7	0.012 4	0.174 9	0.010 5	0.151 7
	Average	0.196 3	0.012 7	0.170 1	0.010 9	0.151 0

mission. Therefore, no correction method is available that is applicable to all types of waters with good accuracy across the spectrum. The exponential fitting method, developed as a new alternative correction method to Case 2 water, is suitable for the original spectra that are nearly linear or exponentially decreasing in the data, excluding one or two algal peak bands of AC9 (such as 650 and 676 nm). It is suitable for correction of data from most ordinary coastal and inland water, which is dominated by algal and mineral sediment water, yellow substances, or combination of the two. The flat method is always used for single-absorption-tube measured water, and the longer the reference band is, the more accurate is the scattering scattering-correction result. The Zaneveld method, which is regarded as the standard scattering correction method, can be suitable for most water types with near-zero absorption in the near-infrared region, such as in Case 1 or clear water. However, because of the non-zero absorption at 715 nm, a_{pg} at longer wavelengths is strongly underestimated by the two regular correction methods (flat and Zaneveld) in Case 2 water, and shorter

wavelengths yield reasonably good results in coastal waters (Röttgers et al., 2013). The Röttgers method, as a new method that develops an empirical relationship using PSICAM data that has no scattering error, evaluates the absorption in coastal waters using AC9 meters by applying scattering corrections to the flat and Zaneveld methods. It could improve the quality of AC9 absorption at longer wavelengths (Röttgers et al., 2013) and be close to the values corrected by other methods in this study at shorter wavelengths, instead of the overestimation at shorter wavelengths in Röttgers' study (Röttgers et al., 2013). The Boss method is applicable to water with temperature or salinity that is outside the normal range and water with little or no algal content, such as the Dead Sea.

5 CONCLUSION

The exponential method in which the scattering contribution is obtained from a power-law fit generated using nonlinear least squares minimization at seven wavelengths (412, 440, 488, 510, 532, 555, and 715 nm) was found to yield reasonable results for

data sets recently collected using different AC9/ACS instruments and including data from an estuary and its adjacent coastal area, an open gulf, an inland lake, and a reservoir. This correction method proved suitable and robust for different types of turbid waters in coastal and eutrophic waters. In inland waters, it did not require the zero-NIR-absorption assumption or that the raw absorption spectra should be exponentially decreasing. The corrected spectra were shifted upwards in the red and NIR regions.

The corrected results obtained using the exponential method were compared with those of the flat, Zaneveld, Röttgers, and Boss methods. The corrected values generated by the exponential method were found to be very close to those of the flat method (variance of average value <20%) and the Zaneveld method (variance of average value >-30%) in the blue-green bands (≤ 600 nm) and smaller than those in the Röttgers method (variance of median value <35%). They are comparable with the results of the spectrophotometer measurements conducted in the laboratory.

The exponential-function assumption improved the AC9 data quality at longer wavelengths and yielded stable results at shorter wavelengths in the coastal and inland waters. However, problems arise that remain to be addressed, which will be the subjects of a further study. For instance, $c_m(\lambda)$ is left uncorrected in the exponential method due to the lack of an appropriate standard scattering correction. In addition, this method should be validated using samples from more water types. The algorithm also requires modification to improve the scattering correction accuracy.

6 DATA AVAILABILITY STATEMENT

The data that support the findings of this study are available from National Ocean Technology Center and Institute of Remote Sensing and Digital Earth but restrictions apply to the availability of these data, which were used under license for the current study, and thus, are not publicly available. The data are however available from the authors upon reasonable request and with permission from the National Ocean Technology Center and Institute of Remote Sensing and Digital Earth.

7 ACKNOWLEDGEMENT

The authors are appreciative to the members of the field sample experiment for their hard work during

the four cruises over the gulf of Liaodongwan (2011), the estuary of Changjiang (Yangtze) River (2012), the lake of Taihu (2013), the reservoir of Guanting (2015). We greatly appreciate the two anonymous reviewers who provided detailed comments to improve the manuscript.

References

- Babin M, Stramski D, Ferrari G M, Claustre H, Bricaud A, Obolensky G, Hoepffner N. 2003. Variations in the light absorption coefficients of phytoplankton, nonalgal particles, and dissolved organic matter in coastal waters around Europe. *Journal of Geophysical Research*, **108**(C7): 3 211, <https://doi.org/10.1029/2001JC000882>.
- Bidigare R R, Ondrusek M E, Morrow J H, Kiefer D A. 1990. In-vivo absorption properties of algal pigments. In: Proceedings of SPIE 1302, Ocean Optics X. SPIE, Orlando, FL, United States. p.290-302.
- Boss E, Gildor H, Slade W, Sokoletsky L, Oren A, Loftin J. 2013. Optical properties of the Dead Sea. *Journal of Geophysical Research*, **118**(4): 1 821-1 829.
- Boss E, Slade W H, Behrenfeld M, Dall'Olmo G. 2009. Acceptance angle effects on the beam attenuation in the ocean. *Optics Express*, **17**(3): 1 535-1 550.
- Bricaud A, Claustre H, Ras J, Oubelkheir K. 2004. Natural variability of phytoplanktonic absorption in oceanic waters: influence of the size structure of algal populations. *Journal of Geophysical Research*, **109**(C11): C11010.
- Doxaran D, Babin M, Leymarie E. 2007. Near-infrared light scattering by particles in coastal waters. *Optics Express*, **15**(20): 12 834-12 849.
- Hoepffner N, Sathyendranath S. 1991. Effect of pigment composition on absorption properties of phytoplankton. *Marine Ecology Progress Series*, **73**: 11-23.
- Kirk J T O. 1992. Monte Carlo modeling of the performance of a reflective tube absorption meter. *Applied Optics*, **31**(30): 6 463-6 468.
- Kirk J T O. 2010. Light and Photosynthesis in Aquatic Ecosystems. 3rd edn. Cambridge University Press, Cambridge. p.49-95.
- Lefering I, Bengil F, Trees C, Röttgers R, Bowers D, Nimmo-Smith A, Schwarz J, and McKee D. 2016. Optical closure in marine waters from *in situ* inherent optical property measurements. *Optics Express*, **24**(13): 14 036-14 052.
- Leymarie E, Doxaran D, Babin M. 2010. Uncertainties associated to measurements of inherent optical properties in natural waters. *Applied Optics*, **49**(28): 5 415-5 436.
- McKee D, Piskozub J, Brown I. 2008. Scattering error corrections for in situ absorption and attenuation measurements. *Optics Express*, **16**(24): 19 480-19 492.
- McKee D, Piskozub J, Röttgers R, Reynolds R A. 2013. Evaluation and improvement of an iterative scattering correction scheme for in situ absorption and attenuation measurements. *Journal of Atmospheric and Oceanic Technology*, **30**(7): 1 527-1 541.
- Mobley C D. 1994. Light and Water: Radiative Transfer in

- Natural Waters. Academic Press, San Diego, USA. p.86-100.
- Moore C C, Zaneveld J R V, Kitchen J C. 1992. Preliminary results from an in-situ spectral absorption meter. *In: Proceedings of SPIE 1750, Ocean Optics XI*. SPIE, San Diego, CA, United States. p.330-337.
- Morel A. 2009. Are the empirical relationships describing the bio-optical properties of case I waters consistent and internally compatible? *Journal of Geophysical Research*, **114**(C1): C01016.
- Mueller J L, Morel A, Frouin R, Davis C, Arnone R, Carder K, Lee Z P, Steward R G, Hooker S, Mobley C D, McLean S, Holben B, Miller M, Pietras C, Knobelspiesse K D, Fargion G S, Porter J, Voss K. 2003. Ocean Optics Protocols for Satellite Ocean Color Sensor Validation, Revision 4, Volume III: Radiometric Measurements and Data Analysis Protocols. National Aeronautics and Space Administration, Washington DC, USA. p.1-31.
- Pegau S, Zaneveld J R V, Mitchell B G, Mueller J L, Kahru M, Wieland J, Stramska M. 2003. Inherent optical properties: instruments, characterizations, field measurements and data analysis protocols. *In: Mueller J L, Fargion G S, McClain C R eds. Ocean Optics Protocols for Satellite Ocean Color Sensor Validation, Volume IV*. National Aeronautics and Space Administration, Washington, DC, USA. p.1-64.
- Pegau W S, Gray D, Zaneveld J R V. 1997. Absorption and attenuation of visible and near-infrared light in water: dependence on temperature and salinity. *Applied Optics*, **36**(24): 6 035-6 046.
- Roesler C S. 1998. Theoretical and experimental approaches to improve the accuracy of particulate absorption coefficients derived from the quantitative filter technique. *Limnology and Oceanography*, **43**(7): 1 649-1 660.
- Röttgers R, Dupouy C, Taylor B B, Bracher A, Woźniak S B. 2014. Mass-specific light absorption coefficients of natural aquatic particles in the near-infrared spectral region. *Limnology and Oceanography*, **59**(5): 1 449-1 460.
- Röttgers R, McKee D, Woźniak S B. 2013. Evaluation of scatter corrections for ac-9 absorption measurements in coastal waters. *Methods Oceanography*, **7**: 21-39.
- Shen Q, Li J S, Zhang F F, Sun X, Li J, Li W, Zhang B. 2015. Classification of several optically complex waters in China using *in situ* remote sensing reflectance. *Remote Sensing*, **7**(11): 14 731-14 756.
- Shi Z Q, Zhang Y L, Cai T F. 2015. Determination of the spectral absorption coefficients of suspended particulate matters in the shallow lakes in the middle and lower reaches of Yangtze river. *Journal of Lake Sciences*, **27**(3): 519-526. (in Chinese with English abstract)
- Sokoletsky L G, Shen F. 2014. Optical closure for remote-sensing reflectance based on accurate radiative transfer approximations: the case of the Changjiang (Yangtze) river Estuary and its adjacent coastal area, China. *International Journal of Remote Sensing*, **35**(11-12): 4 193-4 224.
- Sosik H M, Mitchell B G. 1995. Light absorption by phytoplankton, photosynthetic pigments and detritus in the California Current system. *Deep Sea Research Part I: Oceanographic Research Papers*, **42**(10): 1 717-1 748.
- Sullivan J M, Twardowski M S, Zaneveld J R V, Moore C M, Barnard A H, Donaghay P L, Rhoades B. 2006. Hyperspectral temperature and salt dependencies of absorption by water and heavy water in the 400-750 nm spectral range. *Applied Optics*, **45**(21): 5 294-5 309.
- Sullivan J, Twardowski M, Moore T, McKee D, Röttgers R, Stockley N. 2016. Improving IOP measurement uncertainties for PACE ocean color remote sensing applications. Florida Atlantic University Harbor Branch, USA.
- Tassan S, Ferrari G M. 2002. A sensitivity analysis of the 'transmittance-reflectance' method for measuring light absorption by aquatic particles. *Journal of Plankton Research*, **24**(8): 757-774.
- Tassan S, Ferrari G M. 2003. Variability of light absorption by aquatic particles in the near-infrared spectral region. *Applied Optics*, **42**(24): 4 802-4 810.
- Twardowski M S, Sullivan J M, Donaghay P L, Zaneveld J R V. 1999. Microscale quantification of the absorption by dissolved and particulate material in coastal waters with an ac-9. *Journal of Atmospheric and Oceanic Technology*, **16**(6): 691-707.
- WET Labs Inc. AC Meter Protocol Document (Revision Q). <http://www.seabird.com/sites/default/files/documents/manual-acprotq.pdf&nid=2320>. Accessed on 2017-02-01.
- Ye H P, Li J S, Li T J, Shen Q, Zhu J H, Wang X Y, Zhang F F, Zhang J, Zhang B. 2016. Spectral classification of the Yellow Sea and implications for coastal ocean color remote sensing. *Remote Sensing*, **8**(4): 321.
- Zaneveld J R V, Kitchen J C, Moore C C. 1994. Scattering error correction of reflecting-tube absorption meters. *In: Proceedings of SPIE 2258, Ocean Optics XII*. SPIE, Bergen, Norway. p.44-55.
- Zhang Y L, Gao G, Shi K, Niu C, Zhou Y Q, Qin B Q, Liu X H. 2014. Absorption and fluorescence characteristics of rainwater CDOM and contribution to Lake Taihu, China. *Atmospheric Environment*, **98**: 483-491.
- Zhu J H, Han B, Ye H P, Yang A A. 2014. Preliminary study on the seawater scattering properties in the outside estuary of the Yangtze River. *Acta Optica Sinica*, **34**(S1): s101001. (in Chinese with English abstract)
- Zhu J H, Zhou H L, Li T J, Han B. 2010. Study on applicability of pathlength amplification correction factor with T-R method based on *Chlorella vulgaris*. *Ocean Technology*, **29**(1): 40-45. (in Chinese with English abstract)
- Zhu J H. 2003. The key technique for measuring spectral absorption coefficient of case II water with spectrophotometer. *Ocean Technology*, **22**(1): 34-39. (in Chinese with English abstract)